AUT Journal of Mechanical Engineering

AUT J. Mech. Eng., 10(1) (2026) 29-42
DOI: 10.22060/ajme.2025.24049.6174

Experimental and Numerical Analysis of Electromagnetic Energy Harvester Based on a Vertical Magnetic Cantilever Beam

Elham Ovaysi, Alireza Shooshtari *, Ali Oveysisarabi

Department of Mechanical Engineering, Bu-Ali Sina University, Hamedan, Iran.

ABSTRACT: In this paper, an energy harvesting system is studied, which is modeled as a vertical cantilever beam with a harmonic base and includes magnetic springs, some magnets, and coils converting the mechanical vibrations into electrical energy, and a resistive load that consumes the harvested energy. The governing equations of motion and the induced current flowing in the resistive load are derived based on the Lagrange equations. The model is validated using a manufactured prototype with three different resistive loads to show the effect of viscous damping on the harvested energy. It is proven that the increase of the external resistance leads to the reduction of both the current flowing in the coil and the electromagnetic damping coefficient. Therefore, system dissipations are reduced and output power is increased. Also, for any resistive load, the experiments are repeated for different locations of the magnetic springs, which shows that the proper adjustment of the location of the magnetic springs makes it possible to harvest maximum energy. From experimental results, the output power is finally obtained in the range of $1.8mW$, which is good for low-power applications.

Review History:
Received: Jun. 12, 2021
Revised: May, 10, 2021
Accepted:
Available Online:

Keywords:
Energy Harvesting
Cantilever Beam
Nonlinear Vibrations
Cantilever Beam
Experimental Analysis

1- Introduction

With recent advances in wireless electromechanical systems, sensors can be placed in almost any location and physical condition. These wireless sensors require a built-in power supply, and most of their power is provided by conventional batteries that have a short lifespan and must be replaced periodically. On the other hand, in the long run, replacement, maintenance costs, and the destructive environmental effects of these energy sources seem to be a great challenge [1-4]. Energy extractors are a good alternative to batteries. These devices convert wasted energy in the environment into useful energy (usually electrical energy), and are referred to as new energy converters. Harvesters are very important as they can supply energy for low-consumption devices that work independently [5-9].

One of the most popular sources for energy harvesting is environmental vibrations, such as the vibrations of buildings, vehicle systems, and the vibrations of any structure that is affected by the force of wind and water waves. Electromagnetic [10, 11], electrostatic [12, 13] and piezoelectric [14, 15] are three basic transducer types employed to convert vibrational energy into electrical energy.

In [16], a single beam connected to the sea floor was investigated, in which sea waves can cause the beam to vibrate, and electrical energy was absorbed by the piezoelectric cells embedded on the body of the beam. In [17], an electromagnetic generator was mentioned. According to the cylindrical shape of the device and the presence of coils and magnets embedded inside it, the system was studied analytically and semi-analytically. Depending on the movements or daily activities of the person (walking, sports, etc.), the cylinder carrying the energy picker was shaken, and by moving the magnet in the cylinder chamber, the current was induced in the circuit.

In [18], energy extraction with the help of electromagnetic and piezoelectric converters was studied. In contrast to conventional methods of energy extraction, the concept of transfer and displacement of a single beam was discussed in this study. Experimental tests and ideal conditions to harvest maximum energy from the mechanism were studied for different input frequencies. Experimental results showed the effect of vibrations caused by a fixed base on energy harvesting, and it was observed that the electromagnetic energy harvesting device with harmonic bases has a higher amount of acquired energy. In order to increase the amount of energy harvested based on vibration, an energy harvester consisting of four piezoelectric interlocking beams that are radially around a circular plate was proposed in [19]. In this structure, the ferromagnetic substrates and a permanent magnet in the middle of the energy converter circle were placed.

In [20], a nonlinear vertical beam with a concentrated mass at the end was proposed as an energy harvester. The

*Corresponding author's email: shooshta@basu.ac.ir

transverse vibrations of this beam in the direction of gravity were analyzed. Also, the dynamics of the electromechanical system and the effect of forces on the structure were investigated. A new cantilever beam was studied in [21] to improve the output power of a cantilever beam-based electromagnetic vibration energy harvester. With the help of the ball-screw mechanism, an energy-regenerative vibration absorber was investigated in [22], which can be applicable to harvest energy from vehicle suspensions. In [23], the potentiality of harvesting energy from a vibrational structure based on double cantilever beams was investigated.

An adaptive control method was proposed in [24] to solve the tracking problem for an electromagnetic energy harvester. This mechanism has been studied theoretically. However, from an experimental point of view, the governing equations of the system studied in [24] including equations of motion and electrical equations should be changed, which can subsequently affect the amount of harvested energy. Hence, the purpose of this paper is: 1) to investigate the electromagnetic energy harvesting system proposed in [24] experimentally, and 2) to construct a prototype to validate the new mathematical model. The main contributions of this research are:

- The system studied in this research is the one presented in [24], which consists of a vertical cantilever beam with a harmonic base, magnets, coils, and magnetic springs that can be placed at different heights from the beam base.
- When the beam vibrates, a relative movement occurs between the magnetic tip of the beam and the coils, which leads to a change in the flux passing through the coil. As a result, the induced current flows in the coil. When this induced current passes through a resistive load, electromagnetic damping occurs, which is not considered in [24].
- Compared to [24], due to the current passing through the resistive load and the subsequent occurrence of viscous damping caused by the effect of the electromagnetic mechanism on the energy harvesting structure, a complete mathematical model is presented in this research.
- The magnetic springs and their displacement play an important role in the beam oscillations. Unlike the other works, such as [16-18, 25] and [19, 20, 26], the oscillations of the beam are affected by the location of magnetic springs, and consequently, the amount of harvested energy can be changed.

The rest of this paper is organized as follows: The proposed electromagnetic energy harvester is modeled in Section 2. The effectiveness of the mechanism is evaluated through simulation and experimental results in Section 3. Finally, we conclude this paper in Section 4.

2- Mathematical Modeling

The electromagnetic energy harvester with the configuration of the system presented in [24] is considered as shown in Fig. 1. This mechanism consists of a vertical cantilever beam, the magnetic tip mass, the magnetic springs embedded on the beam body, coils, and a simple electrical circuit including a resistive load, which is connected to the coil. The beam is fixed in the harmonically excited base. When the base is excited and the beam is vibrated, its free end will oscillate. Then, by moving the magnetic tip of the beam into the coil, an electric voltage is induced in the coil according to Faraday's Law of Induction. Meanwhile, by changing the location of the magnetic springs, the displacement of the free end of the beam will be changed, which can affect the amount of harvested energy. The induced voltage, which will be discussed further, is applied to both the external resistance R_L and the internal resistance of the coil R_c. Due to the existence of R_L, the induced current will flow in the electric circuit. In this way, mechanical energy is converted into electrical energy.

2- 1- Governing Equations

In this section, the governing equations of motion have been extracted using the Euler-Lagrange Method. For this purpose, at first, the potential energy U, kinetic energy T and nonconservative work of the system W_d must be computed.

It must be noted that according to the coordinate system, which is shown in Fig.1, it is assumed that the cantilever beam is excited in base only in the y direction, and so its vibration is only a transverse planar vibration in this direction. So, assuming the base excitation is harmonic, the function of base excitation can be written as

$$y(t) = A_e \cos(\omega t), \tag{1}$$

where A_e and ω are the amplitude and frequency of base excitation, respectively. The potential energy of the beam is the sum of the two potential energies U_1 and U_2. The potential energy U_1 consists of the strain potential energy of the beam, the potential energy stored in the springs, the electromagnetic energy stored in the coil, and the magnetic potential energy stored in the magnetic field. So, one can get [27]

$$\begin{aligned} U_1 &= \frac{1}{2}\int_{V_S} E_s c^2 \vartheta(x,t)^2 dV_s + \frac{1}{2} K_t\, a^2 \varphi(x,t)^2 \\ &\quad - \frac{1}{2} L_c \dot{Q}^2 + C_{Bl} \dot{Q}\, w(L,t) \\ &= \frac{1}{2} E_s \int_0^L \int_{A_S} c^2 \vartheta(x,t)^2 dA_s dx + \frac{1}{2} K_t\, a^2 \varphi(x,t)^2 \\ &\quad - \frac{1}{2} L_c \dot{Q}^2 + C_{Bl} \dot{Q}\, w(L,t) \\ &= \frac{1}{2} E_s I_s \int_0^L \vartheta(x,t)^2 dx + \frac{1}{2} K_t\, a^2 \varphi(x,t)^2 \\ &\quad - \frac{1}{2} L_c \dot{Q}^2 + C_{Bl} \dot{Q}\, w(L,t), \end{aligned} \tag{2}$$

where E_S is the elastic modulus, V_S is the beam volume,

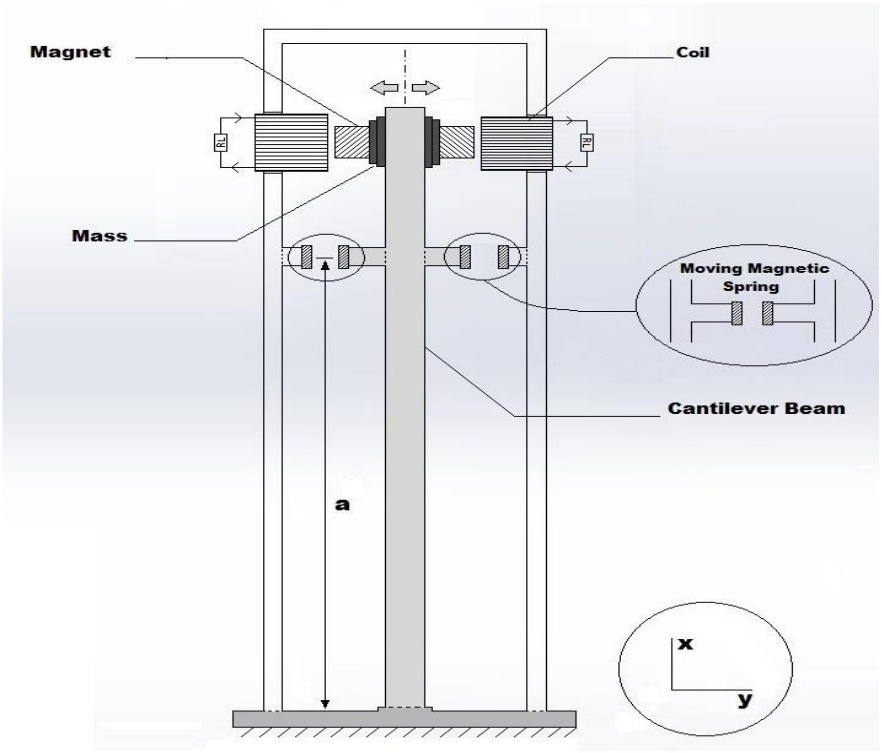

Fig. 1. The electromagnetic energy harvester proposed in [24]

I_S is the second moment of the beam surface, A_S is the beam cross-section, L is the length of the beam, c is the beam thickness, K_t is the equivalent stiffness, a is the magnetic spring height from the base of the beam, L_c is the coil inductance, Q denotes the charge passing through the coil, and C_{Bl} indicates the electromagnetic coupling coefficient, which can be defined as $C_{Bl} = B_{avg}.l_{coil}$ where B_{avg} and l_{coil} represent the average magnetic flux in the coil and the coil's length, respectively [28]. Also, $\varphi(x,t)$ denotes the angle of the beam curvature with respect to the vertical direction, the axes x and y are in the direction of the length and the transverse displacement of the beam, respectively, as shown in Fig. 1. The axes origin is based on the beam. The curvature of the beam in position x and time t is as $\vartheta(x,t)$, and the transverse displacement of the beam is as $w(x,t)$, in which to calculate U_1, we have $x = L$.

The potential energy U_2 represents the gravitational potential energy of the beam with its end masses (i.e. magnets), which can be written as

$$\begin{aligned} U_2 &= -g\int_{V_S} u(x,t)\,dm_s - m_t g u(x,t) = \\ &-g\left(\int_0^L \int_{A_S} \rho_s u(x,t)\,dA_s dx + m_t u(x,t)\right) \\ &= -g\left((\rho_s A_s)\int_0^L u(x,t)\,dx + m_t u(x,t)\right), \end{aligned} \tag{3}$$

where g is the gravity acceleration, ρ_s is the beam density, m_s is the beam mass and m_t is the mass of weights embedded at the end of the beam. The displacement of the beam element in the direction of the x -axis is represented by $u(x,t)$. Note that the mass of the springs is ignored. Also, $m_s = \rho_s V_s = \rho_s A_s x$ and $dm_s = \rho_s\, dA_s\, dx$. Now, the total potential energy of the beam, i.e. U, can be obtained as

$$\begin{aligned} U &= U_1 + U_2 = \frac{1}{2} S_b \int_0^L \vartheta(x,t)^2\,dx \\ &+ \frac{1}{2} K_t\, a^2 \varphi(x,t)^2 - \frac{1}{2} L_c \dot{Q}^2 + C_{Bl}\dot{Q}\, w(L,t) \\ &- g\left(m_b \int_0^L u(x,t)\,dx + m_t u(x,t)\right), \end{aligned} \tag{4}$$

where $S_b = E_s I_s$, and $m_b = \rho_s A_s$, represent the flexural stiffness and mass per unit length of the beam, respectively. Also, $I_s = b\int_{A_S} c^2 dc$, where b denotes the beam width.

The total kinetic energy T is calculated as the sum of the transverse kinetic energy of the beam T_1, the rotational kinetic energy of the beam T_2, and the kinetic energy of the mass embedded at the end of the beam T_3. Now, we get [28]

$$\begin{aligned} T_1 &= \frac{1}{2}\int_{V_S}\left(\left(\dot{w}(x,t)+\dot{y}(t)\right)^2 + \dot{u}(x,t)^2\right) dm_s \\ &= \frac{1}{2}(\rho_s A_s)\int_0^L \left(\left(\dot{w}(x,t)+\dot{y}(t)\right)^2 + \dot{u}(x,t)^2\right) dx, \end{aligned} \tag{5}$$

$$T_2 = \frac{1}{2}\int_{V_S} \dot{\varphi}(x,t)^2 c^2 dm_s = \frac{1}{2}(\rho_s I_s)\int_0^L \dot{\varphi}(x,t)^2 dx = \frac{1}{2} I_b \int_0^L \dot{\varphi}(x,t)^2 dx, \quad (6)$$

$$T_3 = \frac{1}{2}\left(m_t\left(\left(\dot{w}(L,t)+\dot{y}(t)\right)^2 + \dot{u}(L,t)^2\right) + I_0\dot{\varphi}(L,t)^2\right). \quad (7)$$

The total kinetic energy T can be obtained as

$$\begin{aligned} T &= T_1 + T_2 + T_3 \\ &= \frac{1}{2}(\rho_s A_s)\left(\int_0^L \begin{pmatrix} \left(\dot{w}(x,t)+\dot{y}(t)\right)^2 \\ +\dot{u}(x,t)^2 \end{pmatrix} dx\right) \\ &+ \frac{1}{2} I_b \int_0^L \dot{\varphi}(x,t)^2 dx \\ &+ \frac{1}{2}\left(m_t\left(\left(\dot{w}(L,t)+\dot{y}(t)\right)^2 + \dot{u}(L,t)^2\right) + I_0\dot{\varphi}(L,t)^2\right). \end{aligned} \quad (8)$$

According to Fig. 2, $w(x,t)$ is the displacement of the beam element in the direction y which is in the position x and the time t. Also, $\varphi(x,t)$ denotes the direction of the beam element in the position x and time t. The moment of inertia of the tip mass is I_o, and $I_b = \rho_s I_s$ is the moment of inertia of the total beam mass. The Transverse displacement of the beam element is represented as

$$w(x,t) = \sum_{i=1}^{N} q_i \psi_i(x). \quad (9)$$

Assuming that the length of the beam does not change during the vibrations [29], then according to Fig. 2, one can get

$$cos(\varphi) = 1 - \frac{\partial u}{\partial x}, \quad (10)$$

$$sin(\varphi) = \frac{\partial w}{\partial x}. \quad (11)$$

By adding the squares of (10) and (11), we have

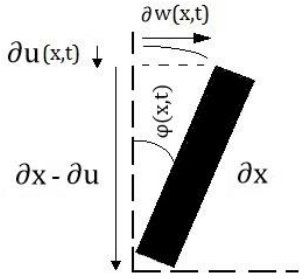

Fig. 2. Beam element in position and time with direction $\varphi(x,t)$

$$(1-\frac{\partial u}{\partial x})^2 + (\frac{\partial w}{\partial x})^2 = 1. \quad (12)$$

Considering (12), and using Pythagorean trigonometric identity in (10) and (11), one can get

$$\begin{aligned} &\frac{\partial u}{\partial x} = 1 - \sqrt{1-\left(\frac{\partial w}{\partial x}\right)^2} \rightarrow \\ &\frac{\partial u}{\partial x} \cong \frac{1}{2}\left(\frac{\partial w}{\partial x}\right)^2 \rightarrow \\ &u(x,t) = \frac{1}{2}\int_0^x \left(\frac{\partial w}{\partial x}\right)^2 dx. \end{aligned} \quad (13)$$

From (11), $\varphi(x,t)$ can be written as

$$\varphi(x,t) = sin^{-1}\left(\frac{\partial w}{\partial x}\right) \approx \frac{\partial w}{\partial x} + \frac{1}{6}\left(\frac{\partial w}{\partial x}\right)^3. \quad (14)$$

According to (14), $\vartheta(x,t)$ can be obtained in terms of $w(x,t)$ as follows

$$\vartheta(x,t) = \frac{\partial \varphi}{\partial x} = \frac{\partial^2 w}{\partial x^2}\left(1 + \frac{1}{2}\left(\frac{\partial w}{\partial x}\right)^2\right). \quad (15)$$

Although several modes are considered in the vibration of the beam, but due to the high excitability of the first mode in the beam vibrations, this mode is considered in the response of this system. So, in (9), $N = 1$ is considered [27, 30]. Hence, $w(x,t)$ is represented by a function of the transverse displacement of the tip mass $q(t)$ through a function for the beam deformation $\psi(x)$, as

$$w\left(x,t\right)=q\left(t\right)\psi\left(x\right), \tag{16}$$

where $\psi(x)=1-cos\left(\frac{\pi x}{2L}\right)$ represents a single shape mode displacement [20]. According to (16), (13)-(15) can be rewritten as

$$u\left(x,t\right)=\frac{1}{2}q^2\int_0^x \psi'\left(z\right)^2 dz\ , \tag{17}$$

$$\varphi\left(x,t\right)=q\psi'\left(x\right)\left(1+\frac{1}{6}q^2\psi'\left(x\right)^2\right), \tag{18}$$

$$\vartheta\left(x,t\right)=q\psi''\left(x\right)\left(1+\frac{1}{2}q^2\psi'\left(x\right)^2\right). \tag{19}$$

Finally, the function $\Phi\left(x\right)$, which describes the cantilever beam modes [20] is defined as

$$\begin{aligned}&\Phi(x)=\cos(\frac{\lambda_r}{L}x)-\cosh(\frac{\lambda_r}{L}x)\\&+\xi_r(\sin(\frac{\lambda_r}{L}x)-\sinh(\frac{\lambda_r}{L}x)),\end{aligned} \tag{20}$$

where ξ_r is a non-dimensional parameter obtained as

$$\xi_r=\frac{sin\left(\lambda_r\right)-sinh\left(\lambda_r\right)}{cos\left(\lambda_r\right)+cos\left(\lambda_r\right)}, \tag{21}$$

and λ_r is the r the eigenvalue of the characteristic equation $1+\cos\left(\lambda\right)+\cos h\left(\lambda\right)=0$.

In addition to calculating the kinetic and potential energy, it is necessary to calculate the nonconservative work W_d, which is divided into two parts. One is the work due to the delivered power to the resistances of the circuit, including the external resistance R_L and the internal resistance of the coil R_c. The other is the work done by the damping force, which includes electromagnetic damping and air damping [28, 31]. Therefore, the nonconservative work W_d can be achieved as

$$\begin{aligned}&W_d=-\frac{1}{2}\left(R_L+R_c\right)\dot{Q}^2\\&-\frac{1}{2}\int_0^L\left(C_m+C_e\right)(\frac{\partial w\left(x,t\right)}{\partial t})^2\,dx\ ,\end{aligned} \tag{22}$$

where C_m is the air damping coefficient, and C_e is the electromagnetic damping coefficient, which is defined later. In fact, the effect of the electromagnetic mechanism on the energy harvesting structure can be modeled as a viscous damping.

Remark 1. Compared with [24], the nonconservative work due to the viscous damping is investigated in this research.

From (16)-(19), the terms of kinetic energy and potential energy can be simplified as

$$\begin{aligned}T&=\frac{1}{2}m_b\left[P_1\dot{q}^2+2P_2\dot{q}\,\dot{\chi}+\dot{\chi}^2L+P_2q^2\dot{q}^2\right]\\&+\frac{1}{2}I_b\dot{q}^2\left[P_4+P_5q^2+P_6q^4\right]\\&+\frac{1}{2}\left(\begin{aligned}&m_t\left[\left(\dot{q}+\dot{\chi}\right)^2+P_4^2q^2\dot{q}^2\right]\\&+I_0\dot{q}^2P_2^2\left[1+\frac{1}{2}P_7^2q^2\right]^2\end{aligned}\right),\end{aligned} \tag{23}$$

and

$$\begin{aligned}U&=\frac{1}{2}S_bq^2\left[P_8+P_9q^2+P_{10}q^4\right]\\&+\frac{1}{2}K_t\ a^2q^2\left[P_7+P_{11}q^2+P_{12}q^4\right]\\&-\frac{1}{2}L_c\dot{Q}^2+C_{Bl}\dot{Q}q-\frac{1}{2}g\left(m_bP_{13}q^2+m_tP_4q^2\right),\end{aligned} \tag{24}$$

where P_1 to P_{13} are defined as

$$\begin{aligned}&P_1=\int_0^L\psi\left(x\right)^2dx\,,\quad P_2=\int_0^L\psi\left(x\right)\,dx\,,\\&P_3=\int_0^L\left(\int_0^x\psi'\left(z\right)^2dz\right)^2dx\,,\\&P_4=\int_0^L\psi'\left(x\right)^2dx\,,\quad P_5=\int_0^L\psi'\left(x\right)^4dx\,,\\&P_6=\frac{1}{2}\int_0^L\psi'\left(x\right)^6dx\,,\\&P_7=\psi'\left(L\right)^2\,,\quad P_8=\int_0^L\psi''\left(x\right)^2dx\,,\\&P_9=\int_0^L\psi''\left(x\right)^2\psi'\left(x\right)^2dx\,,\\&P_{10}=\frac{1}{4}\int_0^L\psi'\left(x\right)^4\psi''\left(x\right)^2dx\,,\\&P_{11}=\frac{1}{3}\psi'\left(L\right)^4\,,\\&P_{12}=\frac{1}{36}\psi'\left(L\right)^6\,,\quad P_{13}=\int_0^L\int_0^x\psi'\left(z\right)^2dzdx\,.\end{aligned} \tag{25}$$

For deriving governing equations of the mechanical and electrical system, the Euler-Lagrange equation is used as follows

$$\frac{\partial}{\partial t}\left(\frac{\partial L_g}{\partial \dot{q}}\right)-\frac{\partial L_g}{\partial q}=\frac{\partial W_d}{\partial \dot{q}}, \tag{26}$$

$$\frac{\partial}{\partial t}\left(\frac{\partial L_g}{\partial \dot{Q}}\right)-\frac{\partial L_g}{\partial Q}=\frac{\partial W_d}{\partial \dot{Q}}, \tag{27}$$

where $L_g = T - U$ is the Lagrangian. Substituting, U and W_d in (26), one can get

$$\frac{\partial}{\partial t}\left(\frac{\partial T}{\partial \dot{q}}\right)-\frac{\partial T}{\partial q}+\frac{\partial U}{\partial q}=\frac{\partial W_d}{\partial \dot{q}} \tag{28}$$

Substituting (22)-(24) in (28), the displacement of the end of the beam is obtained as

$$\begin{aligned}&\left[N_1+N_2q^2+N_3q^4\right]\ddot{q}+N_4q+N_5q^3\\&+N_6q^5+N_2q\dot{q}^2+N_7\dot{q}^2q^3+C_{Bl}\dot{Q}\\&-\left(m_t+P_2m_b\right)A_e\omega^2\cos\left(\omega t\right)+\left(C_m+C_e\right)P_1\dot{q}=0\end{aligned} \tag{29}$$

where N_1 to N_7 are determined as

$$N_1 = m_t + I_bP_4 + m_bP_1 + I_oP_2^2, \tag{30}$$

$$N_2 = m_tP_4^2 + I_bP_5 + m_bP_2 + I_oP_2^2P_7^2, \tag{31}$$

$$N_3 = I_bP_6 + \frac{1}{4}I_oP_2^2P_7^4, \tag{32}$$

$$N_4 = S_bP_8 - gm_bP_{13} - gm_tP_4 + K_ta^2P_7, \tag{33}$$

$$N_5 = 2\left(S_bP_9 + K_ta^2P_{11}\right), \tag{34}$$

$$N_6 = 3\left(S_bP_{10} + K_ta^2P_{12}\right), \tag{35}$$

$$N_7 = 2I_bP_6 + \frac{1}{2}I_oP_2^2P_7^4. \tag{36}$$

Note that $\psi(L)=1$, because the first mode of the beam is considered. Again, substituting U and W_d in (27), one can get

$$\begin{aligned}&-\frac{\partial}{\partial t}\left(\frac{\partial U}{\partial \dot{Q}}\right)=\frac{\partial W_d}{\partial \dot{Q}} \rightarrow\\&L_c\ddot{Q}-C_{Bl}\dot{q}+\left(R_L+R_c\right)\dot{Q}=0 \rightarrow\\&L_c\frac{dI_L}{dt}+\left(R_L+R_c\right)I_L-C_{Bl}\dot{q}=0.\end{aligned} \tag{37}$$

In this way, the electrical equation describing the current passing through the coil, i.e. I_L is obtained according to (37). It should be noted that $\dot{Q}=I_L$.

To obtain dimensionless equations, the change of coordinates as (38) are used [32, 33].

$$\tau=\sqrt{\frac{N_4}{N_1}}t, \quad \frac{d}{dt}=\sqrt{\frac{N_4}{N_1}}\frac{d}{d\tau}, \quad \frac{d^2}{dt^2}=\frac{N_4}{N_1}\frac{d^2}{d\tau^2}. \tag{38}$$

The displacement of the end of the beam can become dimensionless through

$$x=\frac{q}{L}. \tag{39}$$

Now, substituting (38) and (39) in (29), the dimensionless equation for the displacement of the end of the beam is obtained as

$$\begin{aligned}&\left(1+\alpha x^2\right)\frac{d^2x}{d\tau^2}+x+\gamma x^3+\delta x^5\\&+\beta x\left(\frac{dx}{d\tau}\right)^2+\xi_1\frac{dx}{d\tau}+\xi_2I=\Lambda\cos\left(\Omega\tau\right),\end{aligned} \tag{40}$$

where

$$\begin{aligned}&\alpha=\beta=\left(\frac{N_2}{N_1}\right)L^2,\\&\delta=\frac{N_1N_6L^4}{N_4},\\&\gamma=\frac{N_1N_5L^2}{N_4},\\&\xi_1=\frac{(C_m+C_e)P_1\sqrt{\frac{N_4}{N_1}}}{N_4},\end{aligned} \tag{41}$$

$$\xi_2 = \frac{C_{Bl}\sqrt{\frac{N_4}{N_1}}}{LN_4},$$

$$\Lambda = \left(\frac{m_t P_2 m_b}{LN_4}\right) A_e \omega^2,$$

$$\Omega = \frac{\omega}{\sqrt{\frac{N_4}{N_1}}},$$

Now, similar to (40), the electrical equation (37) can also become dimensionless as follows

$$\bar{L}\frac{dI}{d\tau} + \bar{R}I - \bar{C}\frac{dx}{d\tau} = 0, \tag{42}$$

where

$$\bar{L} = L_c \frac{N_4}{N_1}, \tag{43}$$

$$\bar{R} = \left(R_L + R_c\right)\sqrt{\frac{N_4}{N_1}}, \tag{44}$$

$$\bar{C} = C_{Bl} L \sqrt{\frac{N_4}{N_1}}, \tag{45}$$

Note that $\frac{dQ}{d\tau} = I$. In this paper, it is assumed that the geometric dimensions of the beam such as its length are small. Hence, the terms $\frac{N_5}{N_1} L^4 x^3 \left(\frac{dx}{d\tau}\right)^2$ and $\frac{N_3}{N_1} L^4 x^4 \frac{d^2x}{d\tau^2}$ in (40) have been omitted due to their small size.

2- 2- Electromagnetic effect modeling

According to Faraday's Law of Induction, the change in the flux induces an electric current in the coil, which, according to the Lenz's law, the direction of this induced current is opposite to the direction of the inductive force or opposite to the direction of motion of the beam. In this way, by harvesting electrical energy from the system, the oscillation of the system is reduced. That is, when the electric current passes through the coil and the resistive load, an electromagnetic damping is created. The effect of this damping was also applied in the equation of motion (40) and the electrical equation (42). When the current passes through any conductor with resistance, such as a coil, an induced voltage is also created. The voltage induced in the coil can be achieved by Faraday's Law of Induction as

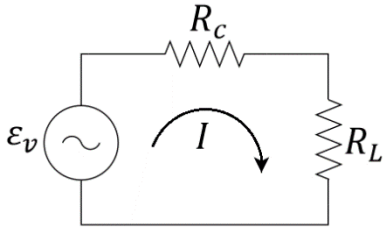

Fig. 3. The equivalent circuit of the harvesting energy mechanism with a resistive load

$$\varepsilon_v = -\frac{d\Phi_B}{d\tau}, \tag{46}$$

where ε_v is the voltage induced, and Φ_B is the magnetic flux. By simplifying (46), we have

$$\varepsilon_v = NBl_{coil}\frac{dx}{d\tau}, \tag{47}$$

where N is the number of turns in the coil, B is the magnetic field, l_{coil} is the length of a winding, and $\frac{dx}{d\tau}$ is the speed of the moving magnets relative to the coil. From this generator, the power P_{out} can be extracted when the coil is connected to a resistive load such as R_L resistance, and then the current flows in the coil. The interaction between the magnetic field created by this current and the magnetic field of the magnets creates an electromagnetic force that opposes the movement (the movement of the free end of the beam inside the coil). The electromagnetic force F_{em} is proportional to the current and subsequently to the speed of movement. Therefore, it can be written as the product of the coefficient

C_e and the speed $\frac{dx}{d\tau}$ as follows [34]

$$F_{em} = C_e \frac{dx}{d\tau}. \tag{48}$$

On the other hand, the electromagnetic force F_{em} can also be written as follows [35]

$$F_{em} = NBl_{coil} I, \tag{49}$$

where I is the induced current flowing in the coil. According to Fig. 3 and Kirchhoff's voltage law (KVL), one can get

$$\varepsilon_v = (R_c + R_L) I \rightarrow NBl_{coil} \frac{dx}{d\tau} = (R_c + R_L) I . \quad (50)$$

Substituting (50) in (49) yields

$$F_{em} = \frac{(NBl_{coil})^2}{(R_c + R_L)} \frac{dx}{d\tau} . \quad (51)$$

Considering (51) and (48), one can get

$$C_e = \frac{(NBl_{coil})^2}{(R_c + R_L)}, \quad (52)$$

where C_e is the electromagnetic damping coefficient. According to Fig. 3, the voltage across the resistance R_L and the output power P_{out} are respectively equal to

$$V_L = \frac{R_L \cdot \varepsilon_v}{(R_c + R_L)}, \quad (53)$$

$$P_{out} = \frac{V_L^2}{R_L} = \frac{R_L \cdot \varepsilon_v^2}{(R_c + R_L)^2} . \quad (54)$$

It should be noted that, the root mean square (RMS) of the output power is defined as

$$P_{RMS} = \frac{V_{L,RMS}^2}{R_L}, V_{L,RMS} = \frac{V_{peak}}{\sqrt{2}}, \quad (55)$$

where V_{peak} is the maximum voltage achieved by (53).

2- 3- Methodology

Numerical results, including the displacement of the free end of the beam, the induced current passing through the coil, the induced voltage, and the voltage across the resistive load, are obtained by solving Eqs (40), (42), (47), and (53). On the other hand, the numerical solution for these equations is provided using the ode-45 method by MATLAB software. Note that the initial conditions for the simulation are selected as $\left[\mathbf{x(0)},\ \frac{dx}{d\tau}\mathbf{(0)},\ \mathbf{I(0)},\ \frac{\mathbf{dI}}{d\tau}\mathbf{(0)}\right] = [\mathbf{0},\ \mathbf{1},\ \mathbf{0},\ \mathbf{0}]$.

The solving time is assumed to be *5s* to achieve solution.

3- Main Results

3- 1- Simulation and Experimental Setup

To validate the obtained equations, a cantilever beam with a concentrated tip mass along with the electromagnetic energy harvester, was simulated by MATLAB platform. A prototype of this mechanism was fabricated. Both theoretical and experimental results are presented in this section. The parameters to design the cantilever beam and electromagnetic harvester are selected according to Table 1, which are almost similar to [24]. The simulation is repeated for different values of the magnetic spring location. The excitation frequency of the beam base is also selected within the range of the natural frequency of the beam. Next, experimental results are presented, and then a comparison between the theoretical and experimental results will be made.

In order to extract the desired voltage, the distance between the magnetic springs and the beam base is adjustable when the system is at rest. With the purpose of harvesting energy, two coils made of twisted copper wire are installed on the body of the structure.

3- 2- Test Procedure

The manufactured prototype is presented in Fig. 4. This structure, including the frame and cantilever beam, is made of Plexiglass material. The beam is fixed at the harmonic base. The tip masses, which are installed at the free end of the beam, are Neodymium magnets.

In order to test and stimulate the beam base, a shaking table is needed. A shaking table based on the Scotch yoke mechanism is proposed and built by the authors. The components of this shaking table, according to Fig. 4, are:

The lower fixed board that is screwed to the work table by graduated grooves.

The support bases, at the end of which the bearings are installed, are connected to the lower fixed board.

The shaking board is placed on the bearings and can move to the left and right.

The Scotch yoke mechanism is connected to the shaking board.

A shaft passes through the support base and connects the mechanism to the shaft of the electric motor (see Fig. 4).

The speed of the electric motor and the rotation rate of the output shaft are kept constant by the dimmer, and the electric motor shaft is also connected to the shaking table by a connector (coupling). According to the scotch yoke mechanism used in the shaking table, after transferring the rotary motion of the electromotor shaft to the shaking table, the shaking board starts moving to the left and right and vibrates whatever is connected to it transversely. After stimulating the beam base by the shaking table, the beam starts to oscillate, and a relative movement occurs between the magnetic tip of the beam and the coils. So, a voltage is induced inside the coil. With the help of an oscilloscope, the induced voltage and the current passing through the resistive load can be observed and measured.

Table 1. Design Parameters for the energy harvester mechanism

Parameter	Value	Parameter	Value
Young's modulus of the beam, E_s	250 GPa	Length of the beam , L	34 cm
Beam density, ρ_s	3×10^4 Kg/m^3	Width of the beam, b	2 cm
Second moment of the beam area, I_s	5×10^{-14} m^4	Electromagnetic coupling coefficient, C_{Bl}	1.33 N/A
Moment of inertia of the tip mass, I_o	3×10^{-3} Kg. m^2	Air damping coefficient, C_m	0.5 N.s/m
Beam mass, m_s	20 g	Length of the coil, l_{coil}	26 m
Cross-sectional area of the beam, A_s	12 mm^2	Cross-sectional area of the coil, A	200 mm^2
Tip mass, m_t	30 g	Number of coil turns, N	600 rpm
Beam thickness, h_s	2.5 mm	Magnetic flux density, B	6×10^{-4} T
Gravitational acceleration, g	9.8 m/s^2	Internal resistance of the coil, R_c	16.8 Ω
Total stiffness, K_t	15 N/ m	Coil inductance, L_c	6.8×10^{-3} H

3- 3- Results and Discussions

In the sequel, the electromagnetic energy harvester is validated through the experimental results. The experiment procedure is as follows: first, a resistive load is connected to the coil and the magnetic Ω

springs are placed at a certain height from the beam base. Then, the base of the beam is excited with a frequency *6 Hz,* and the beam oscillates, and subsequently, the induced voltage and induced current can be measured. Next, with the help of Eq. (55), the output power is calculated. This experiment is repeated for different locations of the magnetic springs and also for three different resistive loads, such as 3Ω , 10Ω and 30Ω. The results are given in the Fig. 5. By trial and error, it is determined that for a resistive load 3Ω, the maximum output power is obtained if the springs are placed at the height of *14 cm*. Similarly, for resistances 10Ω and 30Ω , the maximum output power is obtained when the springs are fixed at heights of *29 cm* and *25 cm*, respectively. Also, the output power in the range of *1 mW* to *2 mW* is suitable for low-power applications such as wireless systems and sensors.

Fig. 6 shows the output power for different excitation frequencies of the beam base, where the resistive load is selected as 30Ω. In Fig. 6, the experiment is repeated for two locations of the magnetic springs as *20 cm* and *25 cm*, and the results are presented. As the excitation frequency increases, the speed of the free end of the beam increases. According to Eq. (47), increasing the speed of the end of the beam leads to an increase in the induced voltage in the coil, which in turn leads to an increase in the output power, according to Eqs. (53) and (54). But this increase in output power is not very significant. Because according to Eq (48), increasing the speed of movement can lead to an increase in electromagnetic force that opposes the movement. Therefore, due to the presence of electromagnetic damping, the voltage across the resistive load and subsequently the output power will not increase much. From Figs. 5 and 6, it is clear that the theoretical and experimental results confirm each other.

It should be noted that in accordance with the dimensions of the vibrating structure, the excitation frequency of the beam base cannot be increased too much because it will lead to damage to the structure. Also, since the tests were conducted on a laboratory scale, the range of output power changes is not very wide.

As shown in Figs. 5 and 6, the effect of 1) the excitation frequency of the beam base, 2) the location of the magnetic springs and 3) the resistive load on the output power, which

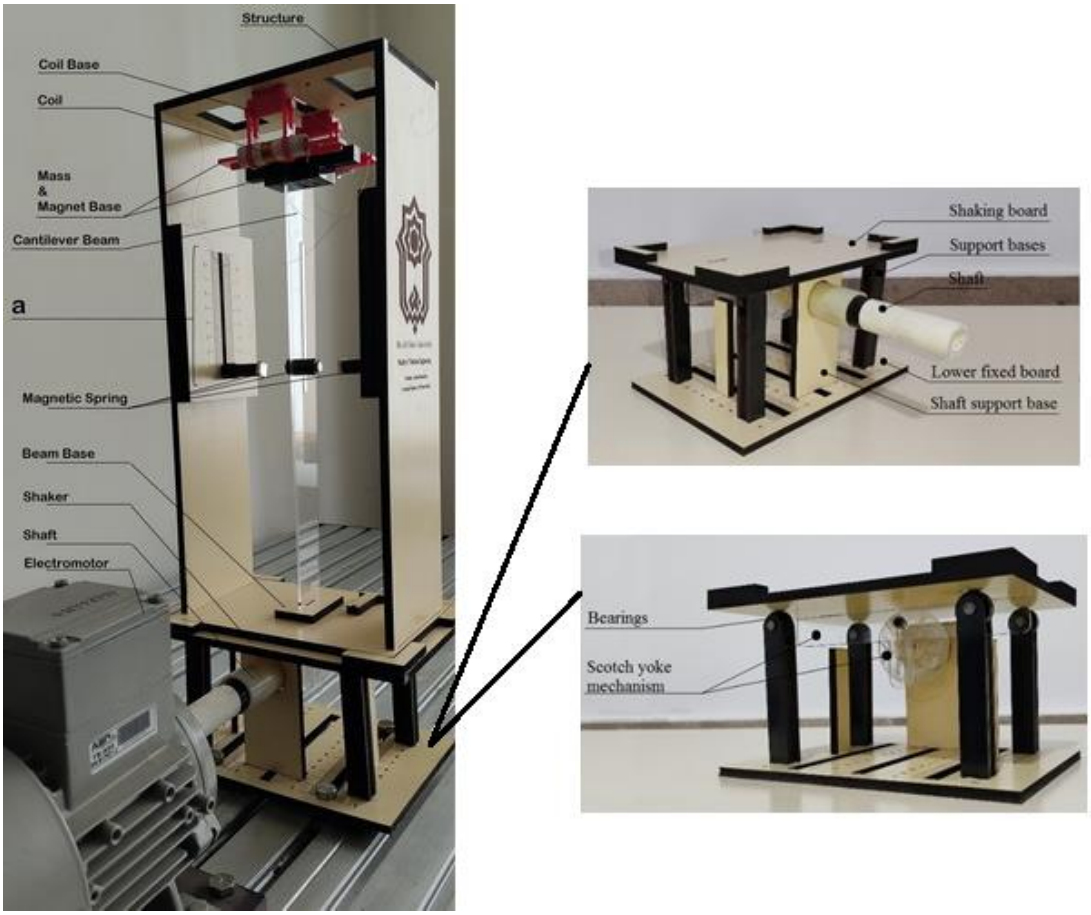

Fig. 4. The constructed experimental prototype

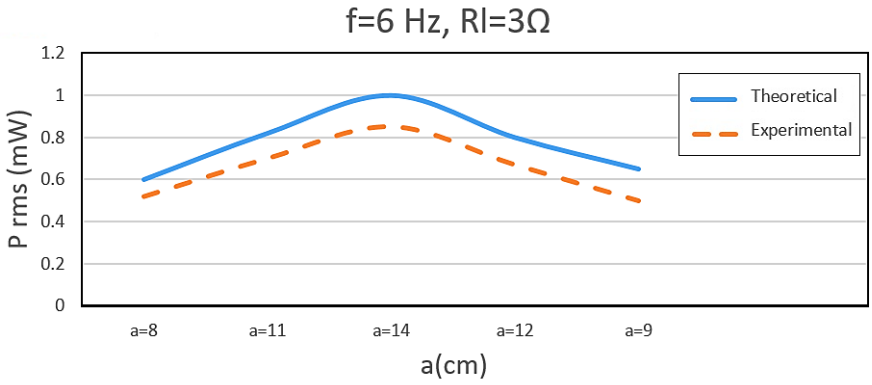

(i)

Fig. 5. The comparison between the theoretical and experimental results for different a. (i) Case $R_L = 3\Omega$, (ii) Case $R_L = 10\Omega$, (iii) Case $R_L = 30\Omega$. (Continued)

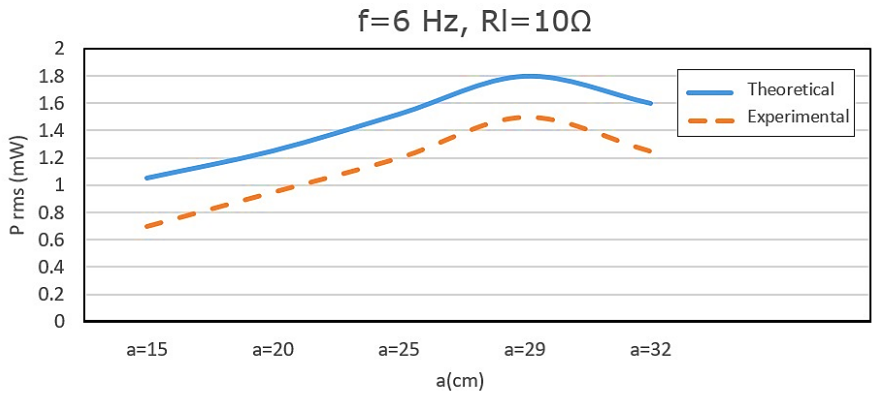

(ii)

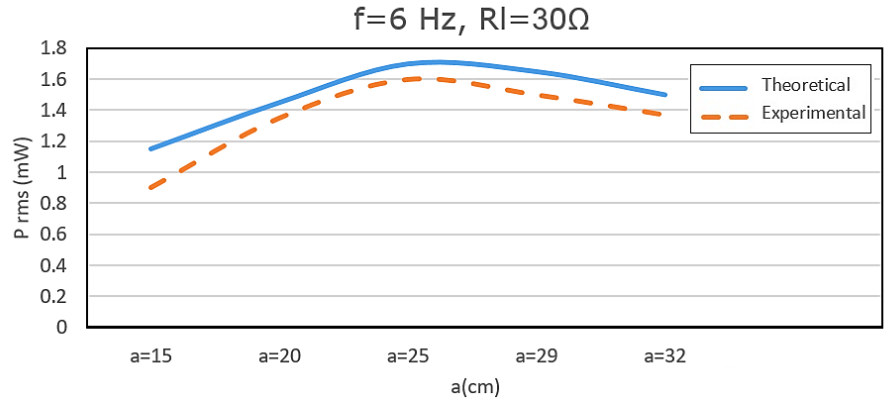

(iii)

Fig. 5. The comparison between the theoretical and experimental results for different a. (i) Case $R_L = 3\Omega$, (ii) Case $R_L = 10\Omega$, (iii) Case $R_L = 30\Omega$.

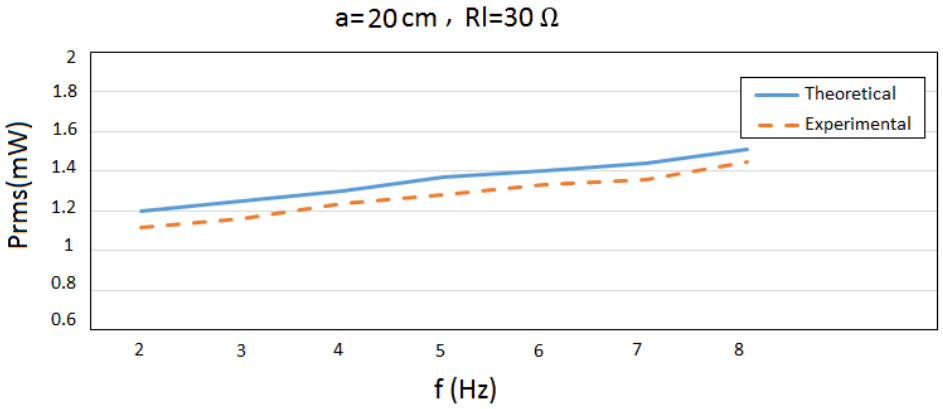

(i)

Fig. 6. The comparison between the theoretical and experimental results for different f. (i) Case $a = 20cm$, (ii) Case $a = 25cm$. (Continued)

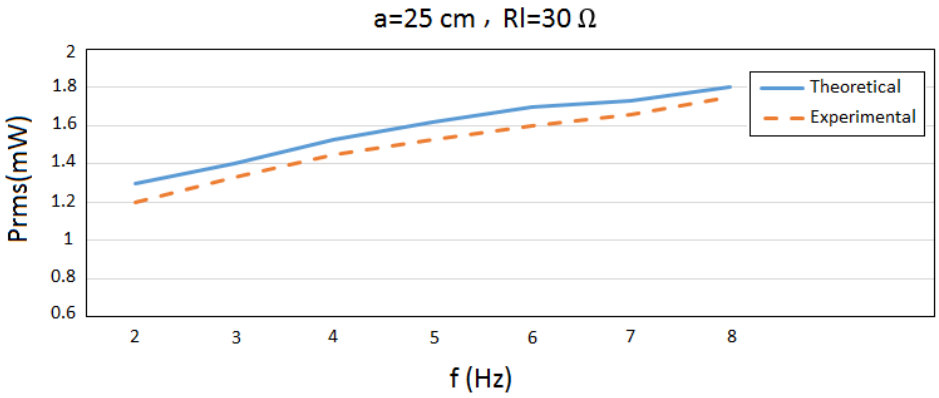

(ii)

Fig. 6. The comparison between the theoretical and experimental results for different f . (i) Case $a = 20cm$, (ii) Case $a = 25cm$. (Continued)

is harvested from the vibrational mechanism are well investigated.

4- Conclusion

This paper investigates an electromagnetic energy harvester consisting of a cantilever beam with a harmonic base, two magnetic springs with changeable location, and some magnets and coils that form the electromagnetic mechanism. In order to harvest energy, a consumer, such as a resistive load, is connected to the system. When current passes through this consumer, a viscous damping occurs in the system, the effect of which is taken into account in the governing equations of the system. These equations are obtained using Lagrange's equations. In addition to analyzing the system by MATLAB, a prototype of the system was built and validated experimentally. The results show that when the resistive load is larger, the current flowing through the coil and the magnetic damping coefficient decrease, which leads to a decrease in system losses and an increase in the harvested energy. By repeating the experiments for different distances of the magnetic springs, it is concluded that for each resistive load, if the location of the springs is properly adjusted, the maximum energy can be extracted. Finally, the results show that the output power is suitable for low-power applications such as wireless systems and sensors. On the other hand, in order to increase the harvested energy, it is suggested that a combination of piezoelectric and electromagnetic transducers be used to harvest energy in future works.

Funding

This work was supported by the Iran National Science Foundation (INSF) under project No.4014249.

References

[1] M.M. Ahmad, F.U. Khan, Review of vibration-based electromagnetic–piezoelectric hybrid energy harvesters, International Journal of Energy Research, 45(4) (2021) 5058-5097.

[2] M. Iqbal, M.M. Nauman, F.U. Khan, P.E. Abas, Q. Cheok, A. Iqbal, B. Aissa, Vibration-based piezoelectric, electromagnetic, and hybrid energy harvesters for microsystems applications: A contributed review, International Journal of Energy Research, 45(1) (2021) 65-102.

[3] Z. Li, C. Xin, Y. Peng, M. Wang, J. Luo, S. Xie, H. Pu, Power density improvement of piezoelectric energy harvesters via a novel hybridization scheme with electromagnetic transduction, Micromachines, 12(7) (2021) 803.

[4] N. Wu, B. Bao, Q. Wang, Review on engineering structural designs for efficient piezoelectric energy harvesting to obtain high power output, Engineering Structures, 235 (2021) 112068.

[5] P. Ibrahim, M. Arafa, Y. Anis, An electromagnetic vibration energy harvester with a tunable mass moment of inertia, Sensors, 21(16) (2021) 5611.

[6] B. Maamer, A. Boughamoura, A.M.F. El-Bab, L.A. Francis, F. Tounsi, A review on design improvements and techniques for mechanical energy harvesting using piezoelectric and electromagnetic schemes, Energy Conversion and Management, 199 (2019) 111973.

[7] A.R.M. Siddique, S. Mahmud, B. Van Heyst, A comprehensive review on vibration-based micro power generators using electromagnetic and piezoelectric transducer mechanisms, Energy Conversion and Management, 106 (2015) 728-747.

[8] C. Ung, S.D. Moss, W.K. Chiu, Electromagnetic energy harvester using coupled oscillating system with 2-degree

of freedom, in: Active and Passive Smart Structures and Integrated Systems 2015, SPIE, 2015, pp. 644-651.

[9] Z. Wang, W. Wang, F. Gu, C. Wang, Q. Zhang, G. Feng, A.D. Ball, On-rotor electromagnetic energy harvester for powering a wireless condition monitoring system on bogie frames, Energy Conversion and Management, 243 (2021) 114413.

[10] M. El-Hami, P. Glynne-Jones, N. White, M. Hill, S. Beeby, E. James, A. Brown, J. Ross, Design and fabrication of a new vibration-based electromechanical power generator, Sensors and Actuators A: Physical, 92(1-3) (2001) 335-342.

[11] S. Meninger, J.O. Mur-Miranda, R. Amirtharajah, A. Chandrakasan, J. Lang, Vibration-to-electric energy conversion, in: Proceedings of the 1999 International Symposium on Low Power Electronics and Design, 1999, pp. 48-53.

[12] S. Roundy, P.K. Wright, K.S. Pister, Micro-electrostatic vibration-to-electricity converters, in: ASME International Mechanical Engineering Congress and exposition, 2002, pp. 487-496.

[13] N.S. Shenck, J.A. Paradiso, Energy scavenging with shoe-mounted piezoelectrics, IEEE micro, 21(3) (2001) 30-42.

[14] P. Glynne-Jones, S. Beeby, E. James, N. White, The modeling of a piezoelectric vibration powered generator for microsystems, in: Transducers' 01 Eurosensors XV: The 11th International Conference on Solid-State Sensors and Actuators, June 10–14, 2001, Munich, Germany, Springer, 2001, pp. 46-49.

[15] Y. Jeon, R. Sood, J.-H. Jeong, S.-G. Kim, MEMS power generator with transverse mode thin film PZT, Sensors and Actuators A: Physical, 122(1) (2005) 16-22.

[16] M. Ettefagh, Reliability Study of Energy Harvesting from Sea Waves by Piezoelectric Patches Considering Random JONSWAP Wave Theory, Journal of Computational Methods in Engineering, 36(2) (2022) 21-34.

[17] P. Carneiro, M.P.S. dos Santos, A. Rodrigues, J.A. Ferreira, J.A. Simões, A.T. Marques, A.L. Kholkin, Electromagnetic energy harvesting using magnetic levitation architectures: A review, Applied Energy, 260 (2020) 114191.

[18] S. Basaran, Hybrid energy harvesting system under the electromagnetic induced vibrations with non-rigid ground connection, Mechanical Systems and Signal Processing, 163 (2022) 108198.

[19] E.F. Haghighi, S. Ziaei-Rad, H. Nahvi, Energy harvesting from a nonlinear magnet-piezoelectric multi-frequency converter array, Smart Materials and Structures, 30(10) (2021) 105028.

[20] M. Borowiec, Energy harvesting of cantilever beam system with linear and nonlinear piezoelectric model, The European Physical Journal Special Topics, 224 (2015) 2771-2785.

[21] F.M. Foong, C.K. Thein, B.L. Ooi, D. Yurchenko, Increased power output of an electromagnetic vibration energy harvester through anti-phase resonance, Mechanical Systems and Signal Processing, 116 (2019) 129-145.

[22] K. Chen, Z. Li, W.-C. Tai, K. Wu, Y. Wang, Mpc-based vibration control and energy harvesting using an electromagnetic vibration absorber with inertia nonlinearity, in: 2020 American Control Conference (ACC), IEEE, 2020, pp. 3071-3076.

[23] R. Eshtehardiha, R. Tikani, S. Ziaei-Rad, Experimental and numerical investigation of energy harvesting from double cantilever beams with internal resonance, Journal of Sound and Vibration, 500 (2021) 116022.

[24] A. Oveysi Sarabi, A. Shooshtari, Adaptive tracking control of a new nonlinear energy harvester system based on the cantilever beam structure, Journal of Vibration and Control, 30(9-10) (2024) 1971-1983.

[25] B. Janizade, M. Dardel, M.H. Pashaei, R.A. Alashti, Investigation of energy harvesting from vibrating nonlinear Timoshenko beam under base oscillating with electromagnetic energy harvester, Modares Mechanical Engineering, 15(1) (2015).

[26] A.S. Hasan, M. Rahman, Multi-level residue harmonic balance method for nonlinear vibration of the beam, Journal of Low Frequency Noise, Vibration and Active Control, 41(1) (2022) 278-291.

[27] M.I. Friswell, S.F. Ali, O. Bilgen, S. Adhikari, A.W. Lees, G. Litak, Non-linear piezoelectric vibration energy harvesting from a vertical cantilever beam with tip mass, Journal of Intelligent Material Systems and Structures, 23(13) (2012) 1505-1521.

[28] H.L. Dai, Y.W. Yang, A. Abdelkefi, L. Wang, Nonlinear analysis and characteristics of inductive galloping energy harvesters, Communications in Nonlinear Science and Numerical Simulation, 59 (2018) 580-591.

[29] A.H. Nayfeh, Linear and nonlinear structural mechanics, John Wiley & Sons, 2024.

[30] [30] S.S. Rao, Vibration of continuous systems, John Wiley & Sons, 2019.

[31] B.A. Owens, B.P. Mann, Linear and nonlinear electromagnetic coupling models in vibration-based energy harvesting, Journal of Sound and Vibration, 331(4) (2012) 922-937.

[32] H. Hatami, A. Fathollahi, Theoretical and numerical study and comparison of the inertia effects on the collapse behavior of expanded metal tube absorber with single and double cell under impact loading, Amirkabir Journal of Mechanical Engineering, 50(5) (2018) 999-1014.

[33] H. Hatami, M.S. Rad, A.G. Jahromi, A theoretical analysis of the energy absorption response of expanded metal tubes under impact loads, International Journal of Impact Engineering, 109 (2017) 224-239.

[34] S.P. Beeby, T. O'Donnell, Electromagnetic energy harvesting, Energy Harvesting Technologies, (2009) 129-161.

[35] H. Lee, M.D. Noh, Y.-W. Park, Optimal design of electromagnetic energy harvester using analytic equations, IEEE Transactions on Magnetics, 53(11) (2017) 1-5.

HOW TO CITE THIS ARTICLE
E. Ovaysi, A. R. Shooshtari, A. Oveysisarabi, Experimental and Numerical Analysis of Electromagnetic Energy Harvester Based on a Vertical Magnetic Cantilever Beam , AUT J. Mech Eng., 10(1) (2026) 29-42.

DOI: 10.22060/ajme.2025.24049.6174